Through Wall Sensing with Multi-Frequency Microwave Radiometry: A Proof of Concept Demonstration

Joel T. Johnson, *Fellow, IEEE*, Metin A. Demir, and Ninoslav Majurec

***Abstract*— A proof of concept demonstration of through wall sensing with microwave radiometry is described. A multi-frequency microwave radiometer with 37 channels from 2.1 to 17.35 GHz was used in two experiments to observe objects through a cinder block wall of approximately 20 cm thickness. Measured data show the clear ability of the radiometer to detect thermal contrasts on the interior of the wall. A discussion of the basic physical processes involved in the measurement is provided. When compared to active systems, microwave radiometry for through wall sensing faces significant challenges, including limitations in ranging, horizontal resolution, and corruption by radio frequency interference, but also provides complementary capabilities particularly with regard to thermal information. Further consideration of microwave radiometry appears warranted for applications where thermal information is of interest.**

***Index Terms*— Microwave Radiometry, Remote Sensing**

I. Introduction

SENSING of building interiors is a topic of current interest due to the wide range of public safety and defense applications. Electromagnetic sensors using microwave frequencies are one of the competing technologies for this purpose, and are useful due to their penetration of building walls while retaining adequate resolution and standoff capabilities. Active microwave sensors (i.e. radars) have been demonstrated extensively [1], and are beginning to reach a reasonable level of maturity in retrieving interior building information, although extensive computations and measurements are required in order to improve retrieval performance.

In contrast, almost no consideration has been given to microwave radiometry for sensing building interiors, primarily due to several limitations of passive methods when compared to active approaches. In particular, passive sensors do not directly obtain range information, but rather measure information that has been integrated over range. Microwave radiometers also have spatial resolutions that are limited by the antenna pattern (i.e. the formation of synthetic apertures is not possible), so that horizontal resolutions can be an issue particularly in standoff geometries. Radiometers also are incapable of directly measuring along range velocity information.

Given these limitations, it may initially appear that further consideration of microwave radiometry is not warranted for through wall sensing. However, radiometry also has certain advantages when compared to radar systems. The primary advantage is the ability of a microwave radiometer to obtain thermal information that is unavailable from active measurements. In addition, a microwave radiometer observes only a one-way path through building walls, as opposed to a two-way path for radar systems, so that attenuation effects are reduced in radiometric observations. Finally, microwave radiometry is completely passive, so that observations are more difficult to detect by the persons or objects being observed.

This paper documents a basic proof-of-concept demonstration of microwave radiometry for through wall sensing. The goal of the paper is simply to demonstrate that microwave radiometer measurements are sensitive to changes in a building interior, and that these changes are consistent with physical expectations.

The next section describes the basic physics of building interior observations with microwave radiometry, followed by a description of the experiments performed and radiometer system utilized. Results from a first and second set of experiments are presented in Sections IV and V, respectively.

II. Physics of through wall observations with microwave radiometry

A microwave radiometer is a receiver designed to measure naturally emitted thermal noise power from the scene under view; the basic physics of microwave radiometry is described in [2]-[3]. Microwave radiometry has been used extensively in remote sensing [2]-[3] as well as in sub-surface sensing applications [4]-[9] and for thermal measurements in medical treatment [10]-[11]. Millimeter wave passive systems have also been considered for a wide range of applications, including most recently airport security screening [12], but such frequencies are less useful for building interior sensing due to the high attenuation through building walls at these frequencies.

Powers measured by a microwave radiometer include the internally generated receiver noise, the noise produced by the radiometer antenna (which includes any antenna loss thermal noise as well as received external noise power), and any radio frequency interference (RFI) in the band due to man-made transmissions. The impact of RFI on radiometry is important, but can be reduced through the use of RFI detection and mitigation algorithms (e.g. [13].) RFI is not considered further in this paper.

The goal of microwave radiometry is to estimate the mean external noise power received; the accuracy of the mean power

Manuscript received Month dd, yyyy; revised Month dd, yyyy. J. T. Johnson and N. Majurec are with The Ohio State University, Dept. of Electrical and Computer Engineering and ElectroScience Laboratory. M. A. Demir was with The Ohio State University and is now with IETR, Rennes, France.

estimation is improved by using long integration times in the measurement and wide frequency bandwidths. Internally generated noise contributions are accounted for through a calibration process in which internal or external sources of a known thermal noise power are measured. The measurements to be described in Sections IV and V use an internal calibration process to determine the observed antenna temperature, which includes any antenna loss contributions as well as the impact of all thermal noise sources within the antenna pattern. Calibration coefficients in this process were determined through separate measurements of ambient and liquid-nitrogen-cooled terminated coaxial cables placed on the radiometer's antenna port.

The antenna temperature measurements obtained are sensitive to the brightness temperatures of any targets observed; the brightness temperature of an object represents the physical temperature of a black body target that would produce a thermal noise power identical to the measured power. Brightness temperatures of homogeneous objects at uniform temperature and in free space are bounded by zero and the physical temperature of the object. The ratio of such an object's brightness temperature to its physical temperature is called its emissivity. The emissivity of an object depends both on its material composition and on its geometry; generally objects that absorb microwave power when illuminated have higher emissivities, while those that reflect microwave power have lower emissivities.

In realistic environments, observed objects both directly emit thermal noise and transmit, reflect, or scatter the thermal noise from other objects into the radiometer's field of view. For through wall sensing applications, the scene under view contains an exterior (or an interior if the sensor is inside the building) wall of a building, with the building interior containing objects on the other side. It is to be expected that building walls at frequencies from 2-18 GHz are likely to be relatively high emissivity objects, given the fact that significant attenuations through building walls are usually observed in radar through wall measurements. Therefore the brightness temperature observed is primarily that of the wall itself (estimated around 70-90 percent of its physical temperature) plus any contributions from thermal sources in the building interior attenuated by the loss through the wall. Particular interior sources should be distinguishable if they have a significant thermal contrast with the surrounding environment inside the building. A clear application of sensing the location of fire inside buildings results. In such situations, changes of the brightness temperature with frequency would be expected to be dominated by changes in the attenuation through the wall. A-priori knowledge of the wall attenuation versus frequency should improve the retrieval of interior thermal information.

Two other mechanisms may also affect through wall observations. The first involves an interference process for layered media when multiple specular reflections are significant [4],[6]. Such interference effects can produce an oscillation in the brightness temperature versus frequency with the oscillatory pattern depending on the distance between the layers. This effect was used to determine the depth of sub-surface targets in [6], and could potentially allow range information

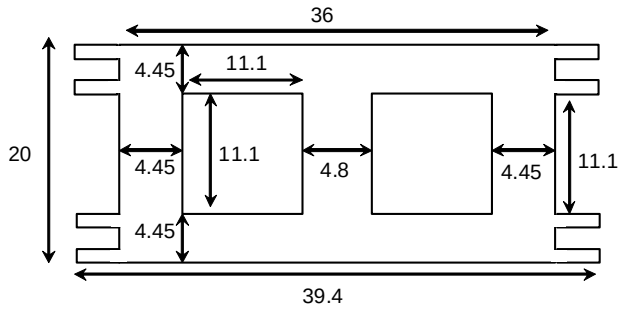

Fig. 1. Approximate cinder block geometry (top view). Dimensions are in cm.

to be determined in through wall measurements if a multiple reflection geometry (e.g. a "flat" object close to the wall) exists. Second, the extent to which any object of interest fills the antenna pattern at a given range will also be an important parameter in the observation, as the measurement is sensitive to a pattern weighted sum of emissions from all objects in the antenna field-of-view. In general, the fact that the spatial resolution of radiometric measurements is limited by the antenna motivates locating the antenna as close to the observed scene as possible. While this raises concerns about near-field effects on the antenna performance, such effects are less influential in radiometry due to the incoherent nature of the measurements performed. Results in Section IV and V will be shown to scale with the fraction of the antenna pattern that an object of interest occupies (i.e. the target influence scales as one over the distance squared to the target.)

III. Description of experiments and radiometer system

Two sets of experiments were performed. The first is a proof-of-concept demonstration in a more realistic, but less controlled, indoor environment, while the second was performed in a more controlled outdoor environment to provide additional verification of the results from the first demonstration. In both experiments, the walls used were constructed of concrete cinder blocks of approximately 20 cm thickness. Such blocks contain hollow cavity regions in the through-wall direction, as illustrated in the top view of Figure 1.

Wideband horn antennas were utilized in both experiments, with the antenna used in the first experiment (aperture dimensions 30 by 50 cm) larger than that used in the second (aperture dimensions 11.4 by 22.8 cm). In both experiments, through wall measurements of the background environment were performed as well as through wall measurements of the background plus a liquid nitrogen cooled absorbing target. This target was constructed by placing microwave absorbing material of dimensions 35.3 cm (width) by 29.2 cm (height) by 21.6 cm inside a styrofoam cooler and pouring liquid nitrogen into the cooler. The brightness temperature of such a target has been shown in the radiometer literature to be approximately equal to the 77 K physical temperature of the liquid

nitrogen [14]. It should be expected that the liquid nitrogen cooled absorber will produce a strong thermal signature, as its presence will obstruct ambient temperature thermal noise contributions from directly behind the absorber. A thermal contrast of approximately 213 K (i.e. from ~ 290 K to 77 K) should result; this contrast would then be attenuated by the wall before being observed by the radiometer. The distance of the target from the wall would also be important because the target at larger distances would occupy a smaller portion of the antenna field of view. Results from these observations will be shown in Sections IV and V.

A. Multi-frequency radiometer

The multi-frequency radiometer (MFRAD) used in these experiments is a standard Dicke switching, direct detection radiometer, with 37 distinct receiver channels from 2.1 to 17.35 GHz. Reference [7] provides a list of the channel frequencies and bandwidths (channel frequencies will also be apparent in the data plots to be shown in Section IV.) Twenty-one of these channels are in the 2.1 to 7.8 GHz band expected to be more useful for through wall sensing applications. Experimental data sometimes showed channels (especially those at 2.1 and 3.4 GHz) to contain RFI contributions; RFI corrupted data were discarded from the results to be shown. The MFRAD enclosure is temperature controlled to maintain calibration stability of the system, and internal noise-generator and reference load sources are also available to further improve stability. Measurements are performed sequentially for a 92 msec duration in each of four states (antenna, external terminator, internal reference load, and noise generator); including switching times, a single radiometer "state" is then output to a data recording computer approximately every 435 milliseconds. Data recorded from multiple radiometer states can then be integrated to attempt to improve radiometer sensitivity; each state represents 92 msec of effective integration time. The data to be shown in the first experiment are averaged over 9 measurements for a total of 0.828 seconds of antenna observation time. Antenna temperature standard deviations in individual frequency channels range from 0.12 to 0.5 K in a manner that is consistent with the varying bandwidths of the channels. Results from the second experiment are averaged over approximately 100 measurements to further improve sensitivity.

IV. First experiment description and results

Results will be shown in this section that qualitatively illustrate passive microwave through wall observations in a realistic indoor environment. Figure 2 illustrates the basic measurement configuration for the first experiment. The 30 cm by 50 cm aperture wideband horn antenna was used with the multifrequency radiometer system to observe objects inside the room temperature (~ 290 K) kitchen of the ElectroScience Laboratory building. The radiometer horn antenna was placed in an adjacent room against the wall of the kitchen.

This experiment provides through wall observations of a realistic building interior, but the complex background environment of the ESL kitchen makes a direct comparison

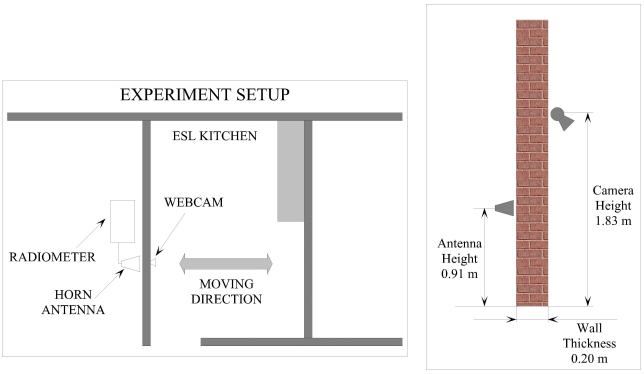

Fig. 2. Experiment setup illustrating top view (left) and side view (right). Moving directions labeled in the left figure indicate that objects within the room were observed at multiple locations.

of measurements with and without the presence of the wall more difficult. The results to be reported in Section V address this issue by performing measurements in a more uniform background outdoor environment.

For the first experiment, the radiometer antenna was placed at a height of approximately 1 m; a video camera was also placed on the interior of the wall in the kitchen in order to record the movements of objects within the room. The kitchen contains several pieces of furniture, a refrigerator, sink, and other objects, all of which remained stationary throughout the measurements. Measurements will be reported for two objects that were moved in the room: the liquid nitrogen cooled microwave absorber located 1 m above the floor and a standing human target. Measurements were performed with these targets either inside or outside the room and at varying distances from the wall. Although measurements were sometimes made as a function of horizontal position within the room, only data with these targets at varying distances normal to the wall and directly in front of the radiometer antenna will be reported. The relatively small antenna aperture at the lower frequencies indicates that the antenna should be sensitive to emission from a wide range of horizontal positions within the room. The liquid nitrogen cooled absorber (located within a styrofoam cooler) was placed on a metallic cart, so that the presence of the cart can also impact the measured data.

A. Liquid nitrogen cooled absorber

Figure 3 describes the approximate set of distances of the liquid nitrogen cooled absorbing target from the kitchen wall used in the experiment. The "frame" quantity used to describe these positions refers to the set of image frames recorded by the video camera inside the kitchen. The experiment involved first moving the target from approximately 1.8 m from the wall up to 0.18 m, followed by a few repeat measurements of the target at similar locations (right hand plot of Figure 3.) The liquid nitrogen target was removed from the room from frames 218 to 295 and during the intervals between positions seven through ten in the right hand plot of Figure 3. The entire video sequence was 600 frames, representing 395 seconds of data. The radiometer acquired data continuously during this period. Motion of the liquid nitrogen target cart was performed by

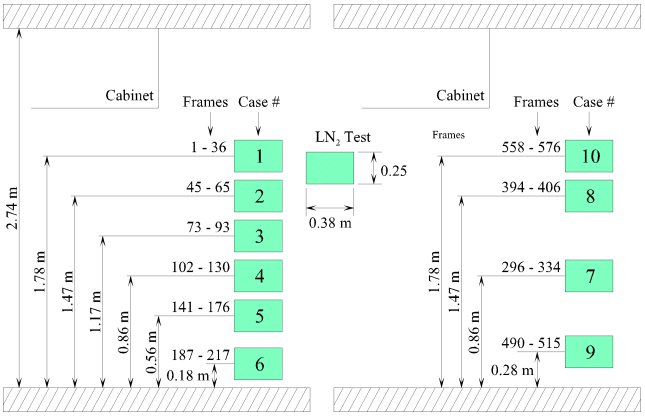

Fig. 3. Description of locations of liquid-nitrogen cooled absorbing target. "Frame" number is used as the "position number" on the horizontal axis of Figures 4 and 5. Right plot positions were performed subsequent to those in the left plot. Target is not in the room during the intervals between positions six through ten.

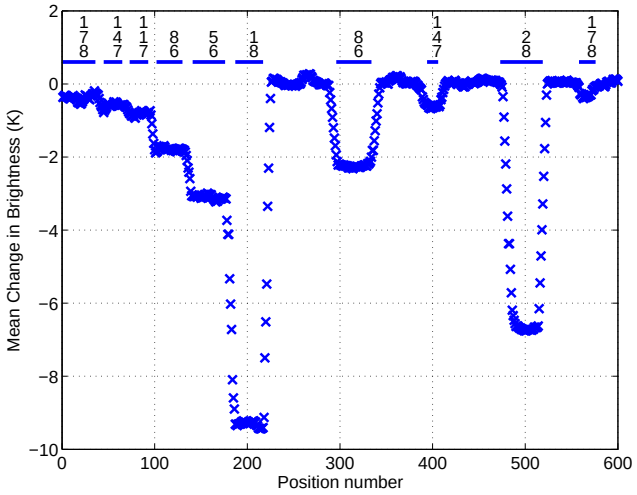

Fig. 4. Change in brightness temperature due to liquid nitrogen cooled absorbing target, averaged over frequencies less than 8 GHz. Distances of target in cm from the wall indicated in upper portion of figure. Figure 3 provides additional information on the relationship between the position number on the horizontal axis and the location of the liquid nitrogen cooled target.

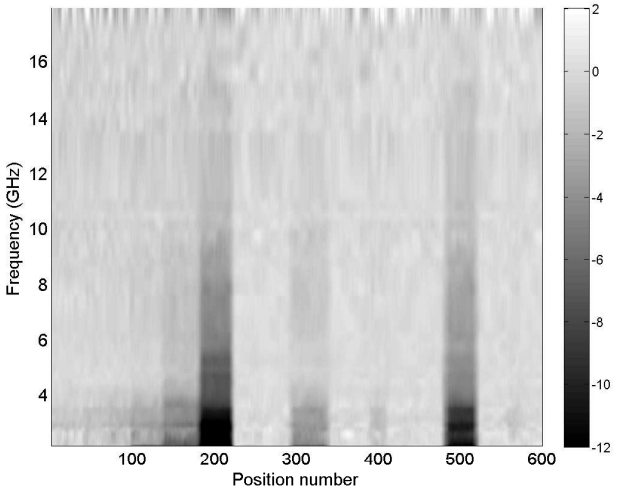

Fig. 5. Spectrogram of brightness temperature changes (in Kelvin) due to liquid nitrogen cooled absorbing target, interpolated to a uniform grid in frequency. Figure 3 provides the relationship between the position number on the horizontal axis and the location of the liquid nitrogen cooled target.

a human operator who entered the room during the periods between the frame locations marked in Figure 3 (e.g. from frames 37 to 44, etc.). No influence of the human operator was observed during the periods when the cart was stationary.

Measured data averaged over the entire time period showed variations versus frequency that are likely related to antenna impedance effects given the strong reflection experienced with the antenna placed directly against the wall. These variations were removed by subtracting the mean over time from each frequency channel's data; the mean over time was computed during a time when the liquid nitrogen target and human operator were not in the kitchen. The average over frequency (using 19 channels from 2.2 to 7.8 GHz) of the resulting changes in brightness temperature is plotted in Figure 4 as a function of time, here represented in terms of the closest camera frame number. Periods of time when the liquid nitrogen cooled target was stationary in the room are indicated by the horizontal lines in the upper portion of the Figure, and the distance of the target from the interior side of the wall in cm is also labeled.

The results clearly show the ability of the radiometer to detect the presence of the liquid nitrogen cooled target, with the frequency-averaged brightness perturbation dropping more than 9 K when the target is at its closest position (frames or position numbers 187-217.) Significant but smaller perturbations are observed when the target is at larger distances from the wall; a measurable change is still observed even with the target at its largest distance (frames 558-576.)

Figure 5 provides an image of the complete dataset versus target position number and frequency; the linearly scaled frequency axis was obtained by interpolating measured data to a uniform 64 point grid in frequency. The results again clearly show the perturbations observed in Figure 4, and also indicate that changes with frequency appear to be consistent with an increased wall attenuation as the frequency is increased. An observable signature is obtained even at frequencies greater than 10 GHz.

Further information on trends versus frequency is provided in Figure 6, which plots the change in brightness versus frequency averaged over positions 187 through 217, when the target was in closest proximity to the wall. The results again suggest that variations in frequency in this case are dominated by an increasing attenuation through the wall as the frequency is increased. A simple exponential curve fit is found to reproduce the measured data reasonably well, although some indication of oscillatory behavior versus frequency is observed in the measured data. Measurable signatures of the liquid nitrogen target are observed even up to 11.4 GHz. A more quantitative analysis of the apparent attenuation through the wall as observed by the radiometer is reported in Section V.

Brightness perturbations averaged over frequency channels less than 8 GHz are plotted versus target distance from the interior side of the wall in Figure 7. The decreasing trend

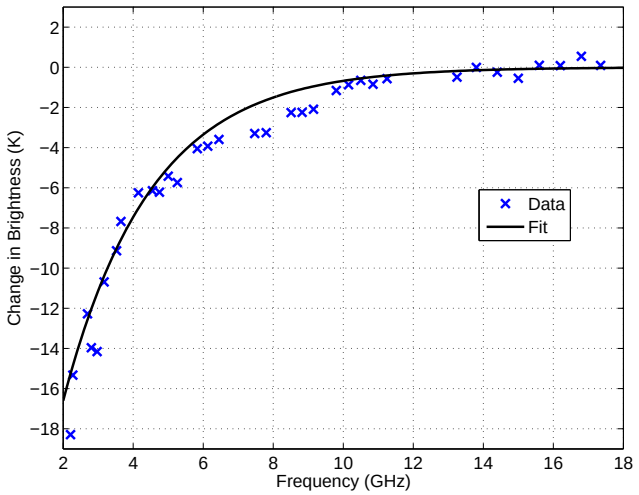

Fig. 6. Change in brightness temperature versus frequency for liquid nitrogen cooled absorbing target with center 0.18 m from the wall. Results are compared to an exponentially decaying curve fit.

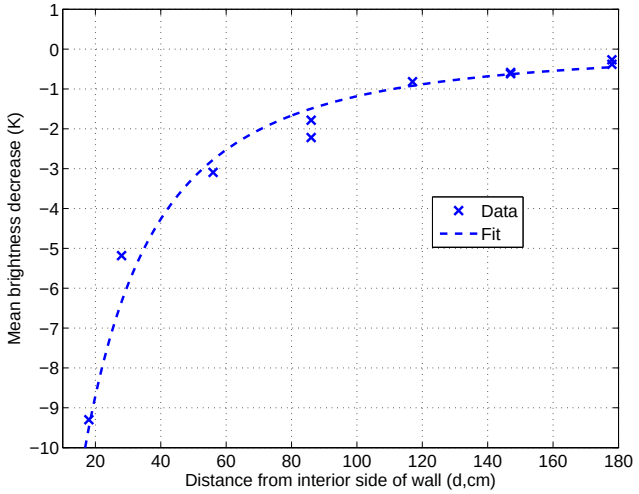

Fig. 7. Change in brightness temperature averaged over frequency channels less than 8 GHz versus distance from interior side of wall for liquid nitrogen cooled absorbing target. Results are compared to a one over distance squared curve fit.

with distance is clearly evident; a curve fit is included using a one over distance squared function, although the distance used is increased from that of the horizontal axis to account for the wall thickness. It was found in this process that the best fit was obtained using an increase of 26.7 cm (curve shown) as opposed to the 20.3 cm thickness of the wall. An increase would be consistent with accounting for a greater phase delay through the wall. In general, the results of this experiment clearly show the capability of a microwave radiometer system for measuring through wall thermal contrasts.

B. Human target

Expectations for radiometric signatures of a human target are more difficult to quantify. The thermal contrast is approximately 14.5 K, but the emissivity of a human target may be lower than that of other objects due to the high dielectric constant of water at microwave frequencies.

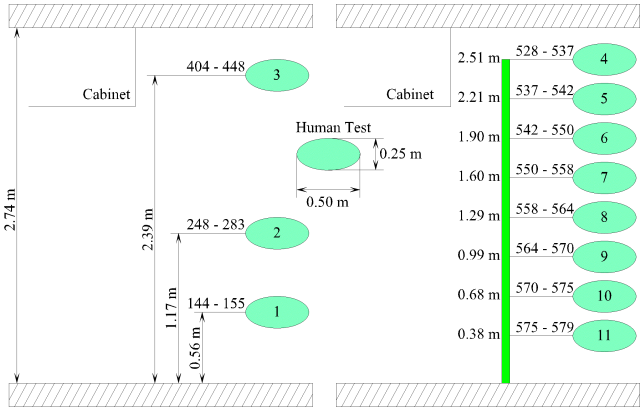

Fig. 8. Description of locations of human target. “Frame” number is used as the “position number” on the horizontal axis of Figures 9 and 10. Right plot positions were performed following those in the left plot, and occurred as a more rapid motion toward the wall. Human target is not in the room during the intervals between target positions one through three in the left hand plot.

Figures 8 through 11 are analogous to Figures 3 through 6 for the human target observations. In this case, the experiment involved observations of the human at distances of 56 cm, 117 cm, and 239 cm from the wall (left plot of Figure 8) followed by a more rapid motion toward the wall from distances of 2.5 m to 38 cm (right plot). The human target was not in the room during the intervals not corresponding to positions one through four in the left hand portion of 8.

The mean over time was again subtracted from each frequency channel in the following datasets. Due to the smaller thermal contrast of the human target, only frequencies less than 8 GHz are used in what follows. The average over frequency of the changes in brightness temperature is plotted in Figure 9 as a function of the closest camera frame number, again with distances to the interior side of the wall indicated in the upper portion of the Figure. Signatures in this case are increases in brightness temperature, and are much smaller than those obtained with the liquid nitrogen cooled target due to the smaller thermal contrast. The results nevertheless show that the human target presence can be observed. Note the averaging operation over frequency further improves the standard deviation of the resulting brightnesses by a factor of approximately 4.3, so that a standard deviation less than 0.1 K is achieved. Signatures again show a consistent decrease as the distance to the target is increased. The final sequence of motion toward the wall is too rapid for the radiometer to resolve individual motions, but shows the expected increasing trend as the distance is decreased.

The complete data image in Figure 10 (interpolated for frequencies less than 8 GHz to a 32 point linear axis in frequency) shows the perturbations observed in Figure 9, but with reduced contrast compared to the liquid nitrogen case. A decreasing trend of the perturbations with frequency is observed.

Brightness perturbations are plotted in Figure 11 versus frequency for distance 56 cm from the wall, and again show an approximate exponential decrease with frequency. An increase in brightness greater than 3 K is observed at the lowest frequencies.

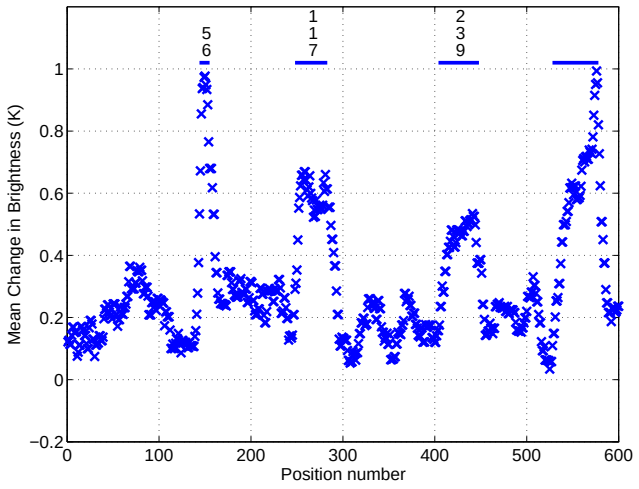

Fig. 9. Change in brightness temperature due to human target, averaged over the frequencies illustrated in Figure 11. Figure 8 provides the relationship between the position number on the horizontal axis and the location of the human target. Human target is in the room during intervals having a horizontal line in the upper portion of the Figure.

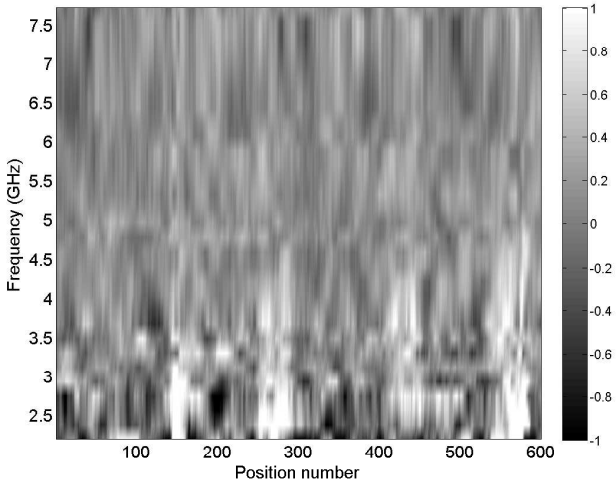

Fig. 10. Spectrogram of brightness temperature changes (in Kelvin) due to human target, interpolated to a uniform grid in frequency. Figure 8 provides the relationship between the position number on the horizontal axis and the location of the human target.

V. Second Experiment Description and Results

The results of the first experiment qualitatively demonstrate the ability of a microwave radiometer to observe thermal contrasts through walls. In order to provide a more quantitative demonstration, a second experiment was performed in an outdoor environment with a more uniform background scene. This scene enables measurements of the absorbing target at ambient temperature and cooled with liquid nitrogen to be more directly compared with and without the wall. In addition, a direct network analyzer measurement of the through wall attenuation (described later) was also performed to provide further information.

These measurements utilized a wideband horn antenna of aperture dimensions 11.4 by 22.8 cm; two identical antennas

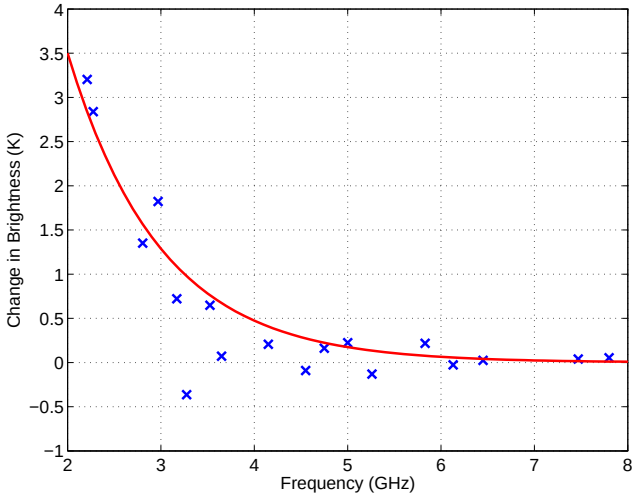

Fig. 11. Change in brightness temperature versus frequency for human target with center 56 cm from the wall. Results are compared to an exponentially decaying curve fit.

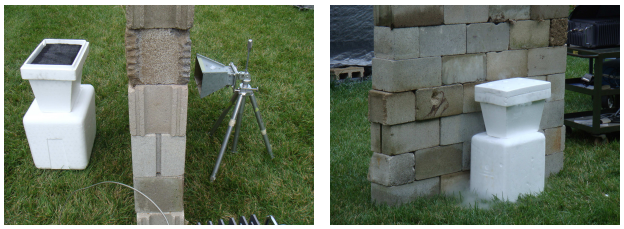

Fig. 12. Photographs of second experiment configuration. Left illustrates wall, radiometer antenna, and absorbing target with base, while right illustrates target with liquid nitrogen at distance 0 cm from the wall.

were used for the network analyzer attenuation measurement. A cinder block wall of dimensions 158.75 cm wide by 19.37 cm thick by 135.9 cm high was constructed using blocks similar to those in the ElectroScience Laboratory building walls (although no mortar or paint was placed on these blocks.) The lower edge of the radiometer antenna was placed at a height of 80 cm above the ground at a distance of 15.25 cm from the wall; the horn antenna aperture was directed normally to the wall.

The microwave absorbing target from the first experiment was placed on the opposite side of the wall at distances ranging from 0 cm to 45.7 cm. In order to eliminate the effect of the metallic cart used in experiment one, the target in this experiment was placed on a cubic styrofoam base of height 48.3 cm. Figure 12 provides photographs of the wall, target, and stryofoam base, as well as the antenna utilized.

Measurements were performed with no target, with the ambient temperature target at varying distances from the wall and with the liquid nitrogen cooled target at the same distances from the wall. This set of measurements was also repeated with the same distances between the radiometer antenna and target with no wall.

Figure 13 plots calibrated antenna temperatures for these datasets versus target distance from the wall at 2.21 (upper

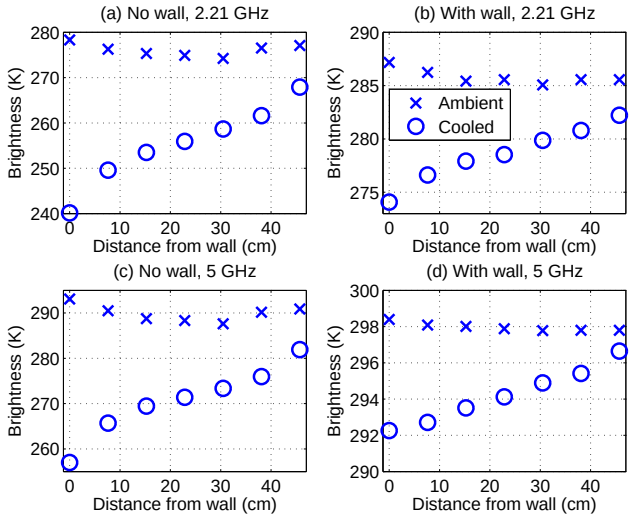

Fig. 13. Calibrated antenna temperatures versus target distance from the wall for ambient and liquid nitrogen cooled absorbing targets. Upper and lower plots are for 2.21 and 5 GHz, respectively. Left and right plots are without and with the wall, respectively.

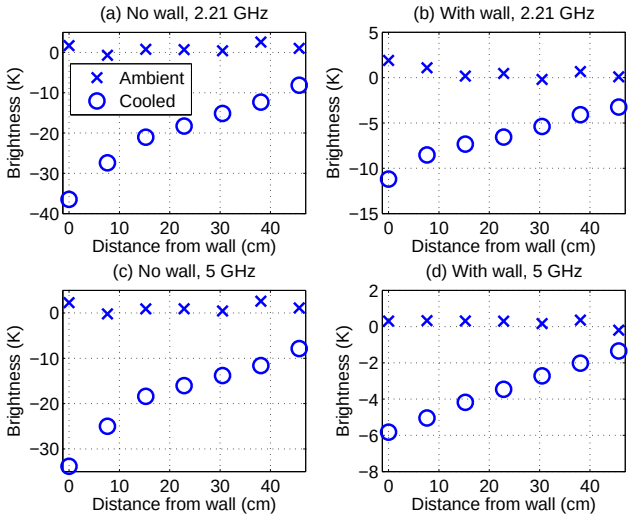

Fig. 14. Same as Figure 13, but with no-target antenna temperatures subtracted.

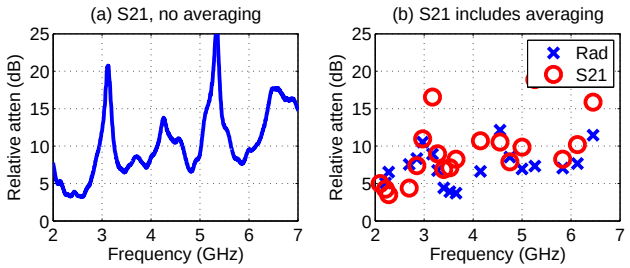

Fig. 15. Network analyzer measured wall attenuation versus frequency (left) and comparison of network analyzer and radiometer estimated attenuation versus frequency (right). Radiometer target or network analyzer receive antenna located at 7.62 cm from the wall.

plots) and 5 GHz (lower plots). The left and right hand side plots respectively are cases without and with the wall. Results for the ambient temperature absorbing target show only very small variations with target distance, due to the fact that the background environment has a brightness temperature similar to that of the ambient temperature target. The cooled target however produces a much stronger change in brightness that is reduced as the target is moved further from the radiometer antenna. Without the wall, a decrease in brightness of approximately 30-40 K is observed with the target at its closest position; these changes are reduced to 6-10 K with the wall. Dependencies on target distance are matched reasonably well by a one over the distance (including the wall thickness) squared function.

Figure 14 is identical to Figure 13 but with the antenna temperatures in the absence of the target subtracted. Such differences provide clearer evidence of the impact of the target, as contributions from background emitters outside the target region should be removed. Again the ability of the radiometer to observe thermal contrasts through the wall is apparent.

An estimate of attenuation through the wall can be obtained from the radiometer by dividing the cooled target brightness differences in Figure 14 in the cases with and without the wall. Such an estimate can then be compared with the attenuation measured by the network analyzer. The network analyzer measurement utilized the radiometer antenna as the transmitter, and an identical antenna as the receiver placed at the same height and at the same set of distances from the wall as the target in the radiometer measurements. Attenuation was estimated with the network analyzer by taking the ratio of calibrated S_{21} measurements with and without the wall for antennas separated by the same distances.

Figure 15 illustrates the network analyzer measured wall attenuation versus frequency in the left hand plot, with the receive antenna located 7.6 cm from the wall. The results show attenuations ranging from 3.2 to greater than 25 dB in an oscillatory pattern over the range of frequencies illustrated. These values are roughly consistent with values reported in the literature at 2 GHz [15]-[16], and oscillatory patterns are also expected due to the layered and periodic geometry of the cinder block wall (see Figure 1). For comparison with the radiometer estimated attenuation, the network analyzer results were power averaged in frequency over bandwidths corresponding to the radiometer channels. The comparison of network analyzer and radiometer estimated attenuations in the right hand plot of Figure 15 shows similar behaviors, and the level of agreement is reasonable given the fact that the radiometer estimate uses only a single antenna while the network analyzer uses two. The oscillatory attenuation behavior observed in experiment two is also consistent with the smaller but similar oscillations in Figure 6 from experiment one.

VI. Conclusions

The results of this study provide a clear proof of concept demonstration for the use of microwave radiometry in through wall sensing measurements. The microwave radiometer essentially can provide, at greatly reduced spatial resolution, a capability similar to that of an infrared camera for heat sensing, but with the possibility of measuring thermal contrasts

through obstructing objects such as the cinder block walls considered here. The results showed that measurable signatures were observed both for strong (liquid nitrogen cooled target) and weak (human target) thermal contrasts. While these results are promising, it is clear that further analysis and experimentation will be required in order to transition such systems into practical applications. One apparent area of application of these ideas could involve the detection of fires or burning objects inside buildings due to the strong thermal contrasts that should be present in such cases.

VII. Acknowledgments

Helpful discussions with several colleagues at the Electro-Science Laboratory are acknowledged, including Drs. Jonathan Young, Robert Burkholder, and Walter D. Burnside. The assistance of James Park, Chun-Sik Chae, and Praphun Naenna with the second set of experiments is also appreciated.

References

[1] Baranoski, E. J, "Visibuilding: Seeing through walls," *IEEE SAM Workshop,* conference proceedings, 2006.

[2] Ulaby, F. T., R. K. Moore, and A. K. Fung, *Microwave Remote Sensing: Active and Passive*, Norwood, MA: Artech House, 1986.

[3] Tsang, L., J. A. Kong, and R. T. Shin, *Theory of Microwave Remote Sensing*, New York: Wiley, 1985

[4] J. T. Johnson, H. Kim, D. R. Wiggins, and Y. Cheon, "Sub-surface object sensing with a multi-frequency microwave radiometer," *IEEE Trans. Geosc. Rem. Sens.*, vol. 40, pp. 2719–2726, 2002.

[5] B. Ungan and J. T. Johnson, "A study of microwave thermal emission from a sub-surface object," *Microwave Opt. Tech. Letters*, vol. 33, pp. 9–12, 2002.

[6] J. T. Johnson, "Theoretical Study of Microwave Radiometry for Buried Object Detection," *SPIE Aerosense meeting: Detection and Remediation Technologies for Mines and Mine-Like Targets*, conference proceedings, vol. 4038, pp. 286–297, 2000.

[7] Johnson, J. T., H. Kim, D. R. Wiggins, and Y. Cheon, "Microwave radiometry for humanitarian demining: experimental results," *Detection and Remediation Technologies for Mines and Minelike Targets VII, Proceedings of SPIE,* 2002.

[8] Peichl, M., Schulteis, S., Dill, S., and Suess H., "Application of microwave radiometry for buried landmine detection," *Proc. of the URSI Symposium on Propagation and Remote Sensing,* conference proceedings, Garmisch-Partenkirchen, Germany, February 2002.

[9] De Amici, G., A. Valles, L. Yujiri, J. Huynh and K. Sherbondy, "Results from field tests of a passive microwave radiometer mine detector," *Detection and Remediation Technologies for Mines and Minelike Targets V, Proceedings of SPIE,* vol. 4038, pp. 262–269, 2000.

[10] H. Ohba, K. Abe, S. Mizushina, S. Mizoshiri, and T. Sugiura, "Recent trends in medical microwave radiometry," *IEICE Tran. Commun.*, vol. E-78-B, pp. 789–798, 2005.

[11] S. Jacobsen and P. R. Stauffer, "Can we settle with single-band radiometric temperature monitoring during hyperthermia treatment of chestwall recurrence of breast cancer using a dual-mode transceiving appplicator?," *Phys. Med. Bio.*, vol. 52, pp. 911–928, 2007.

[12] R. Appleby, R. N. Anderton, S. Price, G. N. Sinclair, and P. R. Coward, "Whole-body 35-GHz security scanner," *Radar Sensor Technology VIII and Passive Millimeter-Wave Imaging Technology VII,* R. Trebits, J. L. Kurtz, R. Appleby, N. A. Salmon, and D. A. Wikner, Eds., vol. 5410, pp. 244 - 251, 2004.

[13] B. Guner, N. Niamsuwan, and J. T. Johnson, "Time and frequency blanking for RFI mitigation in microwave radiometry," *IEEE Trans. Geosc. Rem. Sens.*, vol. 45, pp. 3672–3679, 2007.

[14] Limon, M., C. Marchioni, and G. Sironi, "An absolute cold reference for measurements at UHF and in the microwave band," *J. Phys. E: Sci. Instrumen,* vol. 22, pp. 963–966, 1989.

[15] Wilson, R., "Propagation losses through common building materials," Internal Report, University of Southern California, August 2002. (available at `http://www.am1.us/Papers/E10589%20Propagation%20Losses%202%20and%205GHz.pdf`.)

[16] Taylor, C. D. et al, "On the propagation of RF into a building constructed of cinder block over the frequency range 200 MHz to 3 GHz," *IEEE Trans. Elecmag. Compat.*, vol. 41, pp. 46–49, 1999.